First Principles Study on the Solvation and Structure of $C_2O_4^{2-}(H_2O)_n$, $n = 6-12$

Bing Gao and Zhi-feng Liu*

Department of Chemistry and Centre for Scientific Modeling and Computation, Chinese University of Hong Kong, Shatin, Hong Kong, China

Received: June 3, 2005; In Final Form: July 18, 2005

The structures and energies of hydrated oxalate clusters, $C_2O_4^{2-}(H_2O)_n$, $n = 6-12$, are obtained by density functional theory (DFT) calculations and compared to $SO_4^{2-}(H_2O)_n$. Although the evolution of the cluster structure with size is similar to that of $SO_4^{2-}(H_2O)_n$, there are a number of important and distinctive futures in $C_2O_4^{2-}(H_2O)_n$, including the separation of the two charges due to the C−C bond in $C_2O_4^{2-}$, the lower symmetry around $C_2O_4^{2-}$, and the torsion along the C−C bond, that affect both the structure and the solvation energy. The solvation dynamics for the isomers of $C_2O_4^{2-}(H_2O)_{12}$ are also examined by DFT based ab initio molecular dynamics.

Introduction

Multiple charged anions play important roles in condensed phases for many chemical, physcial and biological processes.[1] They are not very often observed in the gas phase, as the Coulomb repulsion between the excess electrons often leads either to the emission of one electron or to the fragmentation into smaller monoanions.[2−4] Their presence in the condensed phase is due to the stabilizing effects of counterions or solvents. The interactions between these ions and solvent molecules are of fundamental importance in solution chemistry and biochemical reactions. The development of the electrospray ion source has made it possible to produce solvation clusters with a multiple charged anion surrounded by a number of solvent molecules,[5,6] and thus to study the solvation effects in the gas phase. Coupled with mass spectrometry, it has been applied to obtain thermochemistry data[7,8] and to study the dissociation pathways for hydrated anions,[9,10] such as SO_4^{2-}, $S_2O_6^{2-}$, and multiple charged peptide.

Recently, hydrated sulfate and oxalate ions, SO_4^{2-} and $C_2O_4^{2-}$, have also become the first examples for which the electronic structures were probed directly via photodetachment.[11−14] In both cases, a minimum of three H_2O molecules are needed to stabilize the dianion. The measurement provided not only the ionization potential and the repulsive Coulomb barrier but also the trend of structural growth. With the decrease in the intensity of dianion bands, it was identified that the dianion became buried in the cluster as the number of H_2O molecules approached around 12.

The structure of a solvated anion cluster is determined by the delicate balance between anion−solvent and solvent−solvent interactions.[15,16] For hydrated halide ions $X^-(H_2O)_n$, $X = Cl^-$, Br^- and I^-, the anion would stay at the surface for n larger than 4, to maximize the interactions between H_2O molecules.[17,18] On the other hand, F^- could stay either on the surface or the interior of a hydrated cluster with $n = 5$ and 6,[19] due to the strong interaction between F^- and H_2O.

Dianions such as sulfate and oxalate differ in two important aspects with the halide ions in that they are doubly charged and at the same time polyatomic. We have recently studied the solvation of water around SO_4^{2-}, with $n = 6-12$.[20] As expected from the double charge on SO_4^{2-}, the hydrogen bonds in $SO_4^{2-}(H_2O)_n$ are quite strong, and the size of the polyatomic SO_4^{2-} group is such that hydrogen bonds between water molecules attached to separate sulfate oxygen atoms are very extensive. There is thus a hydrogen bonded network among the solvent molecules and the stepwise solvation energy is large, often exceeding 15 kcal/mol for n all the way up to 12. However, the balance between solute−solvent and solvent−solvent interactions remains an important factor for the cluster structure, although the SO_4^{2-} group is always at the center of the cluster, in agreement with experiment.

As a continuing part of our study on the hydrated dianions, we report in this paper the structure and energetics for $C_2O_4^{2-}(H_2O)_n$, with $n = 6-12$. The $C_2O_4^{2-}(H_2O)_n$ clusters with n up to 6 have been examined by ab initio calculations, in combination with photoelectron measurement.[14] Both experimental[11,13,14] and computational results[12,20] on $SO_4^{2-}(H_2O)_n$ indicate that the first solvation around SO_4^{2-} extends beyond $n = 6$. With a slightly larger separation between the two charges and an additional degree of freedom for the internal rotation along the C−C bond, the solvation around $C_2O_4^{2-}$ should be an interesting comparison to SO_4^{2-}. It is also an interesting comparison to dicarboxylate $[CO_2-(CH_2)_n-CO_2]^{2-}$ dianions[21−24] in which the two charges are well separated.

Computational Method

We employed the density functional theory based ab initio molecular dynamics (AIMD) method[25−28] to sample the cluster structure and simulate the solvation dynamics, using the program VASP (Vienna Ab Initio Simulation Package).[29−32] The exchange-correlation energy is calculated by the gradient corrected PW91 functional.[33] The cluster ion is put in a periodic cubic box with a length of 15 Å to minimize the interaction between neighboring cells. A uniform background charge is applied to neutralize the ionic negative charge. The electronic wave function and density are expanded in a planewave basis set, with a cutoff energy of 396 eV, whereas the atomic core region is represented by optimized Vanderbilt ultrasoft pseudopotentials.[34−36] Only the Γ point is used for the k-space sampling. Such a setup makes it possible to perform AIMD simulations at finite temperatures,

* Corresponding author. E-mail: zfliu@cuhk.edu.hk.

10.1021/jp052968t CCC: $30.25
Published on Web 09/17/2005

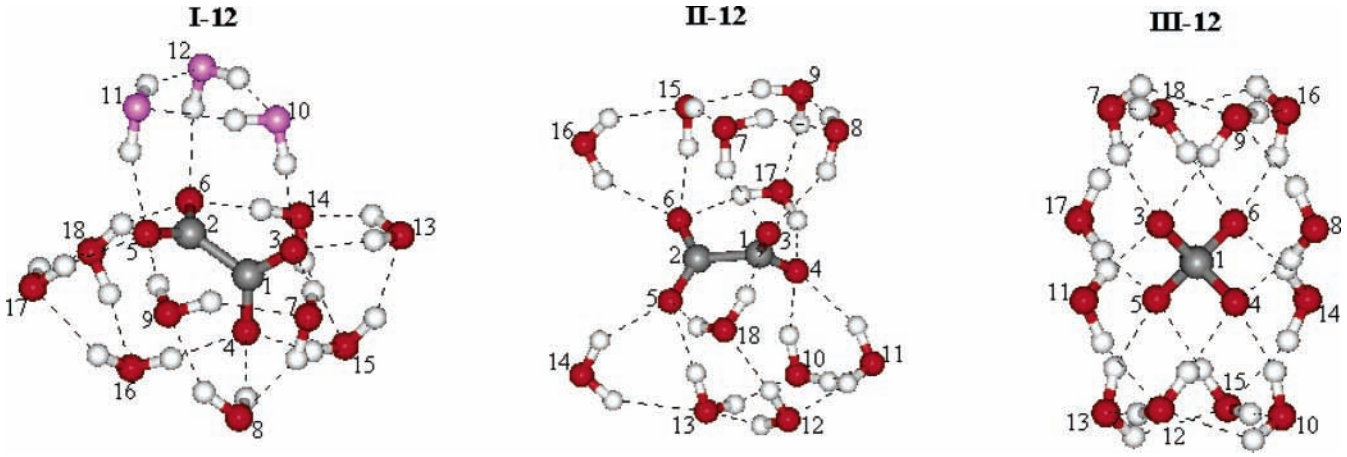

Figure 1. Isomer structures for $C_2O_4^{2-}(H_2O)_{12}$, with the broken lines indicating hydrogen bonds. The lighter color in **I-12** highlights the $(H_2O)_3$ ring.

TABLE 1: Optimized Geometry Parameters for $C_2O_4^{2-}(H_2O)_{12}$ in Series I−III, with Bond Lengths in Å, Bond Angles and Torsion Angles in Degrees

	I-12		II-12		III-12	
C1−C2	1.54		1.55		1.54	
C1−O3	1.27		1.27		1.27	
C2−O6	1.27		1.27		1.27	
∠O3−C1−O4	126.43		125.86		125.39	
∠O5−C2−C1	116.63		116.59		117.31	
torsion	82.1		88.2		81.0	
(a) Representative Hydrogen Bonds between Oxalate Anion and Water Molecules						
O3−H25	1.92		O3−H21	2.05	O3−H19	1.83
O4−H21	1.99		O3−H41	2.01	O3−H27	2.13
O5−H27	1.96		O4−H27	2.06	O4−H21	2.13
O6−H29	1.99		O4−H39	1.93	O4−H30	1.93
			O5−H33	2.06	O5−H31	1.83
			O5−H42	2.05	O5−H39	2.13
			O6−H35	1.83	O6−H42	1.93
			O6−H40	2.14		
(b) Representative Hydrogen Bonds between Water Molecules						
O10−H30	1.98		O8−H20	1.93	O7−H14	1.88
O11−H26	2.09		O10−H32	1.88	O12−H28	2.11
O12−H28	2.00		O15−H38	2.14	O13−H29	1.88
			O17−H24	1.91	O15−H34	2.11
			O18−H30	1.90		

with the total energy and atomic forces calculated at each MD time step from first principles. In such simulations, the time step used is 0.4 fs, and the temperature is controlled by a Nóse-Hoover thermostat,[37,38] with the conservation of the total energy, including the kinetic and potential energy for both the cluster and the thermostat, carefully checked. These trajectories also provide the initial geometry for structural optimization.

Further structural optimizations are performed by using the Gaussian 98 program,[39] at the B3LYP/6-31+G** level, providing the geometries to obtain the energetic values by single point energy calculations with an expanded basis set of AUG-cc-pVDZ and the same B3LYP functional. The basis set superposition error (BSSE) is corrected by the counterpoise correction scheme. The vertical ionization energy is taken as the difference in total energy between the dianion and the monoanion, both at the optimized dianion geometry.

Results and Discussion

a. Cluster Structures for $C_2O_4^{2-}(H_2O)_{12}$. Similar to our previous work on $SO_4^{2-}(H_2O)_n$, we start with the cluster $C_2O_4^{2-}(H_2O)_{12}$, because $n = 12$ was identified as a significant dividing line in the evolution of photoelectron spectra with increasing cluster size.[11] For $SO_4^{2-}(H_2O)_{12}$, the distribution of water molecules around the SO_4^{2-} was found to be symmetric for the most stable isomers, with three H_2O per sulfate O atom. It is worthwhile to examine whether the same applies to the $C_2O_4^{2-}$ ion, which also contains four O atoms. A number of stable isomers were obtained by optimizing structures randomly selected from an AIMD run on $C_2O_4^{2-}(H_2O)_{12}$. The three most stable structures are shown in Figure 1, and their energy difference is within 6 kcal/mol. A number of optimized geometry parameters for these structures are listed in Table 1.

For structure **I-12**, all 12 H_2O molecules are in the first shell, which can be divided into four equivalent groups. In each group, there are three H_2O in a cyclic ring of $(H_2O)_3$, and the remaining O−H bonds are pointed at the same direction to solvate the negatively charged oxalate O atoms. A similar structure was previously reported for $SO_4^{2-}(H_2O)_{12}$.[20] Each O atom on the dianion accepts three hydrogen bonds from three different ring groups. Each H_2O molecule also forms three hydrogen bonds, one donator and one acceptor bond within the same ring group, and one donator bond to a dianion O. Such a structure reaches the maximum number of hydrogen bonds, and the typical bond distances are shown in Table 1. Although this structure is only the second most stable isomer for $SO_4^{2-}(H_2O)_{12}$, it is the most stable isomer for $C_2O_4^{2-}(H_2O)_{12}$.

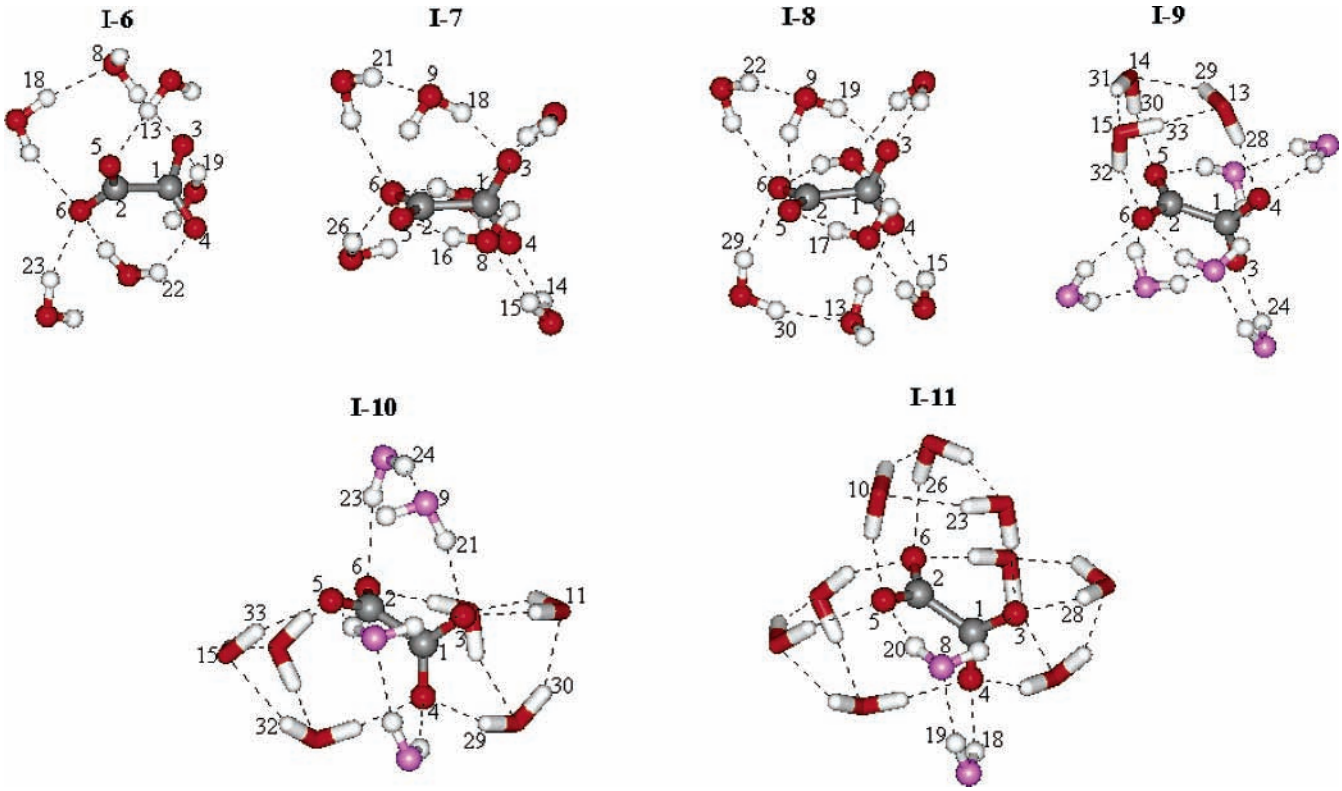

Figure 2. Structures for $C_2O_4^{2-}(H_2O)_n$, $n = 6-11$, in series I, which were obtained by taking away a H_2O molecule successively from **I-12** shown in Figure 1. The $(H_2O)_3$ rings are shown as sticks, and the two H_2O subunits are shown as ball-and-sticks and presented with a lighter color in **I-9**, **I-10**, and **I-11**, to highlight the difference from the $(H_2O)_3$ ring in the same structures. By **I-8**, there is no longer an $(H_2O)_3$ ring.

Slightly higher in energy than **I-12** by only 0.3 kcal/mol is a less symmetric and more complex structure **II-12**. However, a symmetry element is still visible, with a C_2 axis through the two C atoms. It is also obvious that C1−O3−O4 is a dividing plane, with half the twelve H_2O molecules on each side. The hydrogen bonds are less symmetric. On each side, there is one H_2O molecule (O9 and O12) in the second solvation shell. Within the first shell, each of the two H_2O on O17 and O18 takes up a bridge position and donates two hydrogen bonds to two oxalate O atoms. Each of the other eight first shell H_2O molecules donates one hydrogen bond to oxalate, and overall, each oxalate O atom still accepts three hydrogen bonds. Except for the two H_2O molecules on O14 and O16, all other H_2O molecules are saturated with three hydrogen bonds.

The third isomer **III-12** is more than 5 kcal/mol higher in energy than the other two. There are two rings of $(H_2O)_4$, similar to the $(H_2O)_3$ ring in **I-12** and to the $e^-(H_2O)_4$ structure.[40,41] The ring on top solvates O3 and O6 on $C_2O_4^{2-}$, and the ring on the bottom solvates O4 and O5. Then there are two H_2O on each side of the cluster. The structure is again highly symmetrical and each oxygen atom on the oxalate ion accepts three hydrogen bonds. Each H_2O molecule in **III-12** donates one hydrogen bond to $C_2O_4^{2-}$, and thus all H_2O molecules are in the first solvation shells. The hydrogen bond distances between H_2O molecules show considerable variations, as shown in Table 1.

Compared to SO_4^{2-}, $C_2O_4^{2-}$ has an additional degree of freedom, the torsion angle along the C1−C2 bond. For the structure of naked $C_2O_4^{2-}$, as optimized at the B3LYP/TZVP+ level, the torsion angle is 90°, and the solvation interaction with H_2O molecules with $n = 1-6$ produces a substantial decrease in the torsion angle, to as low as 54°.[14] For the three isomers of $C_2O_4^{2-}(H_2O)_{12}$ shown in Figure 1, the torsion angle is 82.1°, 88.2° and 81.0°, respectively, which are only slightly reduced from 90°. It indicates that with 12 H_2O molecules and their symmetric distribution around $C_2O_4^{2-}$, a favorable solvation interaction can be achieved without significant distortion along the C1−C2 axis.

The $C_2O_4^{2-}$ ion can be considered as an intermediate between the dicarboxylate dianion $CO_2^--(CH_2)_n-CO_2^-$ and the sulfate SO_4^{2-} ion. On one hand, the charge separation in $C_2O_4^{2-}$ is much shorter than that in $CO_2^--(CH_2)_n-CO_2^-$,[22−24] and there are extensive hydrogen bonding interactions between H_2O molecules on the two CO_2 groups. On the other hand, the two charges are more separated than the charges on SO_4^{2-} and the space around the $C_2O_4^{2-}$ is less crowded. It accounts for the fact that, whereas for $C_2O_4^{2-}(H_2O)_{12}$ all the H_2O molecules are in the first solvation shell in the most stable structure **I-12**, for $SO_4^{2-}(H_2O)_{12}$ there are eight H_2O in the first shell and four in the second shell in its most stable structure. Nonetheless, the position of $C_2O_4^{2-}$ is at the center of $C_2O_4^{2-}(H_2O)_{12}$, similar to the case of $SO_4^{2-}(H_2O)_{12}$. We have also optimized a number of structures for $C_2O_4^{2-}(H_2O)_{12}$ with n larger than 12 by adding more H_2O to the three isomers shown in Figure 1. In all cases the number of first shell H_2O does not exceed 12.

b. Cluster Structures for $C_2O_4^{2-}(H_2O)_n$, $n = 6-11$. With an electrospray ion source, the small clusters are produced from the larger clusters by the evaporation of solvent molecules. It is thus interesting to identify the weak links in these structures. Using each of the three $C_2O_4^{2-}(H_2O)_{12}$ structures shown in Figure 1 as the starting geometry, we produce a structural series for the smaller clusters with $n = 6-11$, by removing one H_2O molecule in successive steps. At each step, several trials are made by removing a H_2O at different locations, and the series shown in Figures 2−4, are the most stable structures at a particular size and step.

Series I, shown in Figure 2, is generated from **I-12** with one H_2O removed from one of the $(H_2O)_3$ ring groups, which

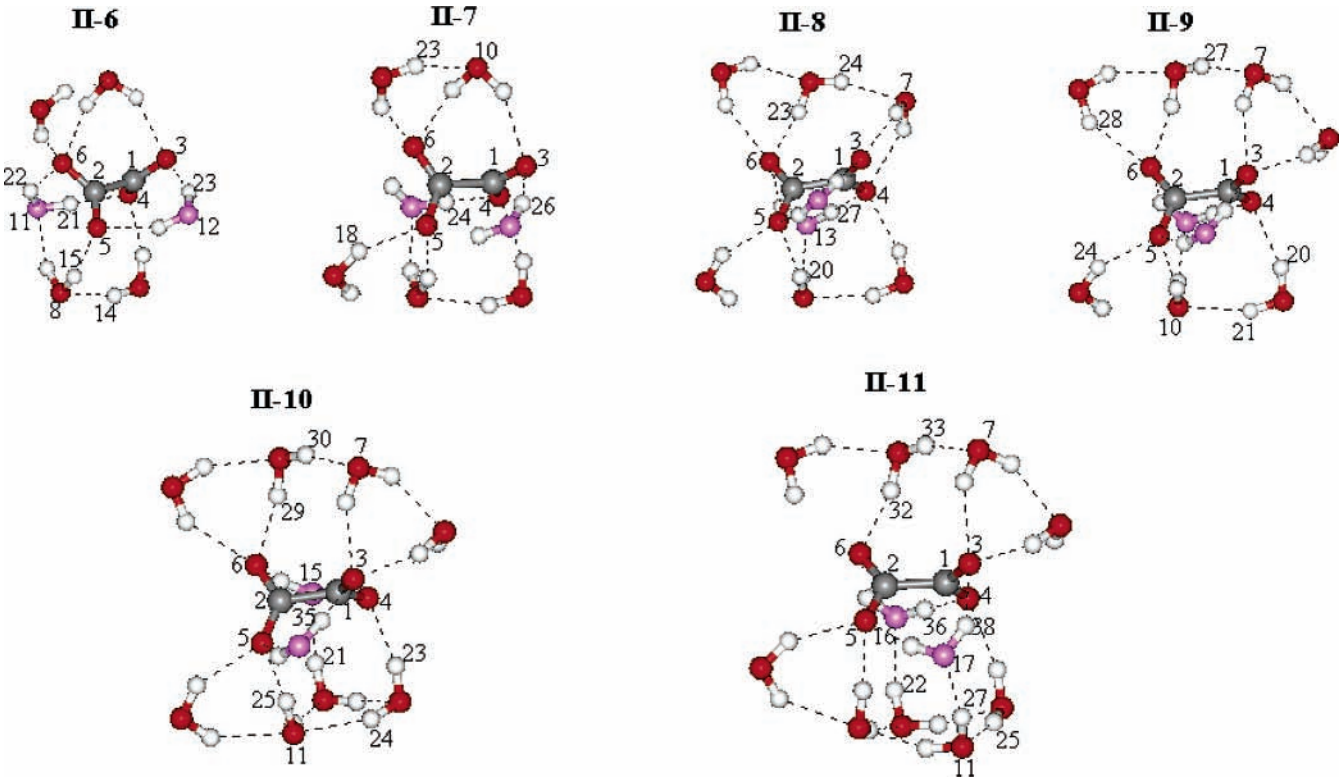

Figure 3. Structures for $C_2O_4^{2-}(H_2O)_n$, $n = 6-11$, in series II, which were obtained by taking away a H_2O molecule successively from **II-12** shown in Figure 1. There are always two H_2O molecules as bidentate hydrogen bond donors to the $C_2O_4^{2-}$ ion, which are highlighted by a lighter color.

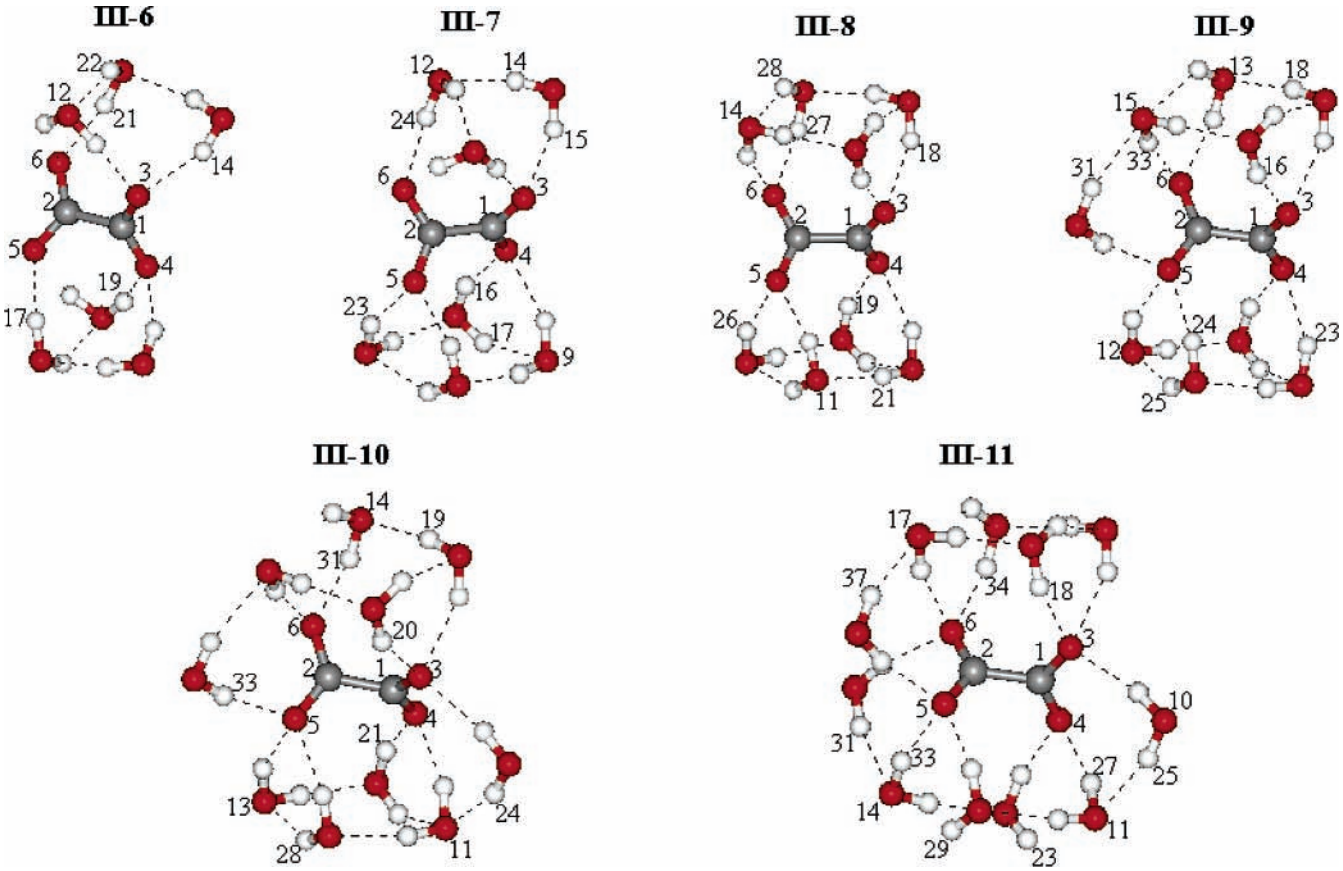

Figure 4. Structures for $C_2O_4^{2-}(H_2O)_n$, $n = 6-11$, in series III, which were obtained by taking away a H_2O molecule successively from **III-12** shown in Figure 1.

becomes a two H_2O group, as one of the H_2O acts as a bidentate hydrogen bond donor to two oxalate oxygen atoms, whereas the other H_2O molecule donates only one hydrogen to an oxalate oxygen and the other hydrogen to the first H_2O in the same

TABLE 2: Calculated Energetic Values for $C_2O_4^{2-}(H_2O)_n$, with $n = 6-12$

	relative energy (kcal/mol)[a]			IP (eV)			ΔE (kcal/mol)[b]			ΔE_s (kcal/mol)[c]		
n	I	II	III	I	II	III	I	II	III	I	II	III
6	2.7	1.4	0	1.46	1.49	1.60	15.7	14.5	15.7	−0.8	−1.7	0.2
7	3.1	3.2	0	1.89	1.87	1.76	15.2	13.7	15.6	−2.7	−2.5	9.0
8	4.4	4.0	0	2.18	2.23	1.93	14.0	14.6	15.3	1.0	−0.5	18.0
9	3.2	3.8	0	2.48	2.53	2.26	14.7	13.6	13.4	2.2	0.6	17.3
10	1.3	2.9	0	2.71	2.71	2.60	13.6	13.6	12.7	7.9	6.2	16.7
11	0.4	0	2.4	2.92	2.83	2.93	14.1	16.1	10.8	13.8	18.2	14.3
12	0	0.3	5.6	3.12	3.00	3.24	13.2	13.2	10.2	19.8	23.9	12.2

[a,b] Stepwise solvation energy, as defined in eq 1. [c] Solvent interaction energy, as defined in eq 2. All three terms (a, b, c) are BSSE corrected, using the coounterpoise scheme.

group for hydrogen bonding. This pattern is maintained until *n* reaches 9, and afterward hydrogen bonds between H_2O molecules produce a more complicated structural pattern.

Series II, shown in Figure 3, starts from the low symmetry structure **II-12**. There are two H_2O molecules (O17 and O18 in Figure 1) in **II-12** as bidentate hydrogen bond donors to two oxalate oxygen atoms. The removal of one of them produces the most stable isomer at $n = 11$, **II-11**, for this series. And, interestingly, there are again two bidentate H_2O molecules (O16 and O17 in Figure 3) in **II-11** after structural optimization. This pattern is repeated through series II to $n = 6$.

For series III (Figure 4), the H_2O molecules are removed in two stages, starting from **III-12**. In the first stage, the two four-H_2O ring are kept, whereas the $(H_2O)_4$ molecules on the two sides are removed successively. By $n = 8$, only the two $(H_2O)_4$ rings are left. For *n* below 8, one H_2O is removed from each of the four H_2O rings successively. This series maintains a fairly regular and clearly identifiable structural pattern. As shown in Table 2, the structure in this series is also the most stable among the three series for $n < 11$, although the energy difference is within 5 kcal/mol.

Our structures of $C_2O_4^{2-}(H_2O)_6$ are slightly different from that obtained by Wang et al.,[14] which is actually 1.4 kcal/mol lower in energy than **6-III**. It indicates that, even at $n = 6$, there are many different structures that are close to each other in energy, and that the structures obtained in such an evaporation procedure are not necessarily the lowest in energy.

c. Solvation Energy. We define the stepwise solvation energy as

$$\Delta E = E[C_2O_4^{2-}(H_2O)_{n-1}] + E[H_2O] - E[C_2O_4^{2-}(H_2O)_n] \quad (1)$$

with both $C_2O_4^{2-}(H_2O)_n$ and $C_2O_4^{2-}(H_2O)_{n-1}$ belonging to the same structural series. The calculated values are listed in Table 2. For $n < 8$, ΔE is around 15 kcal/mol, which indicates fairly strong solvation interaction. As *n* increases over 8, ΔE decreases, which is in agreement with the general trend observed for other hydrated clusters. Fluctuation in ΔE is small, in contrast to the case of $SO_4^{2-}(H_2O)_n$, for which ΔE fluctuates from 7 to 24 kcal/mol in the same size range.

For hydrated anions, the cluster structure is determined by the balance between solute−solvent and solvent−solvent interactions. A similar balance is also evident for $C_2O_4^{2-}(H_2O)_n$, as indicated by the solvent−solvent interaction energy, ΔE_s, defined as

$$\Delta E_s = nE[H_2O] - E[(H_2O)_n] \quad (2)$$

in which the $(H_2O)_n$ has the same geometrical structure as $C_2O_4^{2-}(H_2O)_n$, except that the $C_2O_4^{2-}$ group is removed.

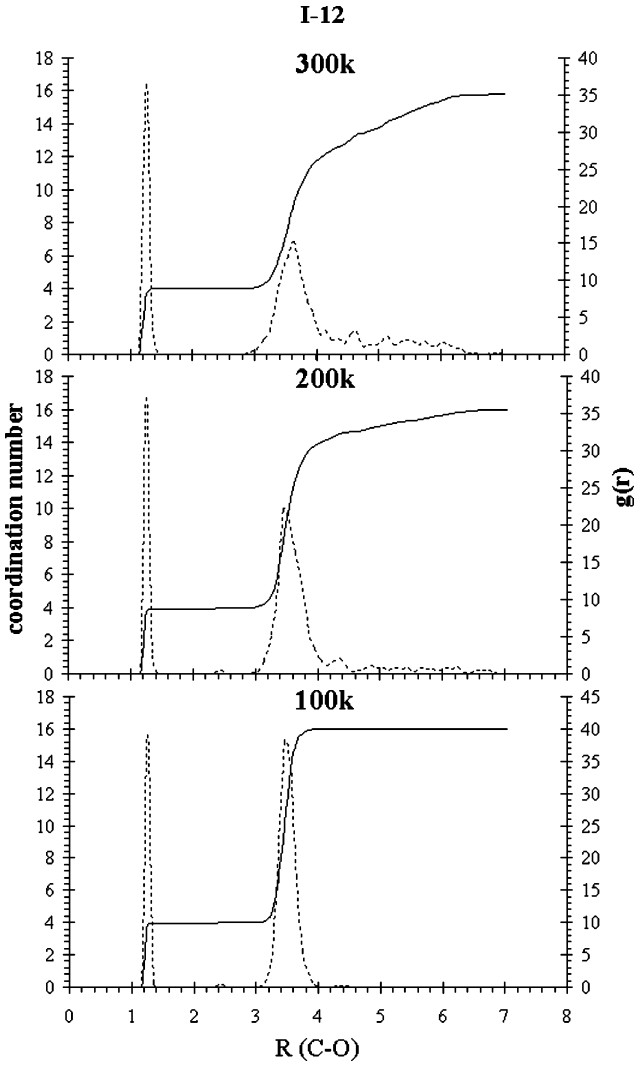

Figure 5. Radial distribution function of oxygen atoms around the carbon atoms for **I-12**, as obtained from ab initio molecular dynamics simulation.

For both series I and II, the value of ΔE_s is small or even negative for *n* below 10, which indicates that solute−solvent interaction is favored. In contrast, more favorable solvent−solvent interaction is achieved in series III, which indicates a better balance between solute−solvent and solvent−solvent interactions and explains the observation that structures in series III are the most stable for $n \leq 10$. For $n > 10$, more favorable solvent−solvent interaction is achieved among all three series.

Within the crowded space around SO_4^{2-}, both solute−solvent and solvent−solvent interactions are strong, and one kind of interaction is often satisfied at the cost of less favorable geometry for the other kind, as indicated by the range of ΔE_s

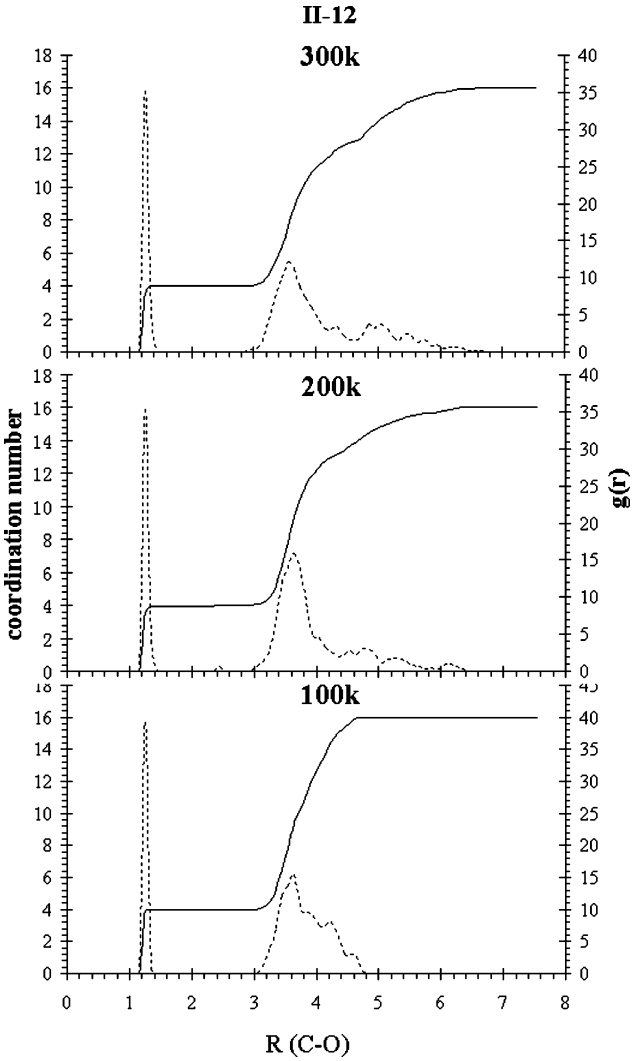

Figure 6. Radial distribution function of oxygen atoms around the carbon atoms for **II-12**, as obtained from ab initio molecular dynamics simulation.

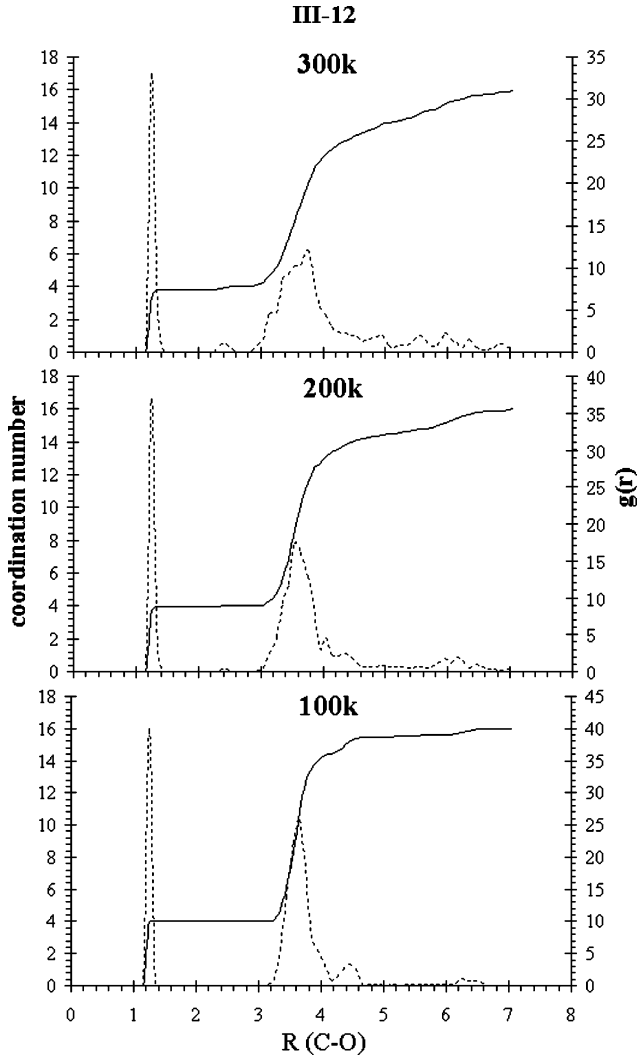

Figure 7. Radial distribution function of oxygen atoms around the carbon atoms for **III-12**, as obtained from ab initio molecular dynamics simulation.

value from −10 to more than +30 kcal/mol.[20] Correspondingly, significant fluctuation in the value of the stepwise solvation energy is observed for $SO_4^{2-}(H_2O)_n$. In contrast, the two charges on $C_2O_4^{2-}$ are more separated, which provides more space to accommodate solvent−solvent interactions. The minimum ΔE_s for $C_2O_4^{2-}(H_2O)_n$ as listed in Table 2 is only −2.7 kcal/mol, and correspondingly, the variation in the stepwise solvation energy is also smoother than that for $SO_4^{2-}(H_2O)_n$.

d. Electronic Structure. The first ionization potentials as calculated by the energy difference between $C_2O_4^{2-}(H_2O)_n$ and $C_2O_4^{-}(H_2O)_n$ at the same geometry are shown in Table 2. For all three structural series, the IP increases with the cluster size. Natural population analysis is also performed for all the structures reported, and the calculated atomic charges show no significant change among these clusters. The two carbon atoms are positively charged, with a value around +0.75. The four oxalate oxygen atoms are negatively charged, with a value of ∼−0.8 each. The overall charge on the $C_2O_4^{2-}$ group is ∼−1.8. The HOMO is always located on the $C_2O_4^{2-}$ group.

e. Solvation Dynamics. The structures shown in Figures 1−4, as obtained by energy minimization, are static structures, whereas, at finite temperature, the solvents would fluctuate considerably in their positions, because the clusters are bound only by hydrogen bonds. Studies on hydrated magnesium dication, $Mg^{2+}(H_2O)_n$, show that there is a "crowding out" of first shell solvents at raised temperatures and a H_2O molecule is squeezed out of the first shell due to the entropy factor.[42,43] Similar effects have also been observed for $SO_4^{2-}(H_2O)_{12}$ in our previous report, and for $C_2O_4^{2-}(H_2O)_{12}$, by ab initio molecular dynamics simulations.

For each of the structures, **I-12**, **II-12**, and **III-12**, we have performed simulations at 100, 200, and 300 K for 2 ps, and the radial distribution functions of oxygen atoms around the carbon atoms are shown in Figures 5−7. **I-12**, with all 12 H_2O molecules falling into four $(H_2O)_3$ groups in the first shell, is the most stable. As shown in Figure 5, there are two well-defined peaks at 100 K, the first peak around 1.2 Å for four the oxalate O atoms, and the second peak around 3.4 Å for all 12 H_2O molecules. At 200 K, the second peak is broadened, due to larger fluctuation, but the $(H_2O)_3$ groups are maintained throughout the simulation. Further broadening is observed at 300 K, and an examination of the trajectory shows that some of the $(H_2O)_3$ are broken. The number of first shell H_2O molecules is reduced to less than 12, indicating the onset of "crowding out".

For **II-12**, the basic structure as shown in Figure 1 is maintained at 100 K, although the peak for H_2O molecules is broad due to the fact that this structure is lower in symmetry than the other two. At 200 K and above, the structure is scrambled, and one could observe the formation of $(H_2O)_3$ and $(H_2O)_4$ rings during part of the simulation.

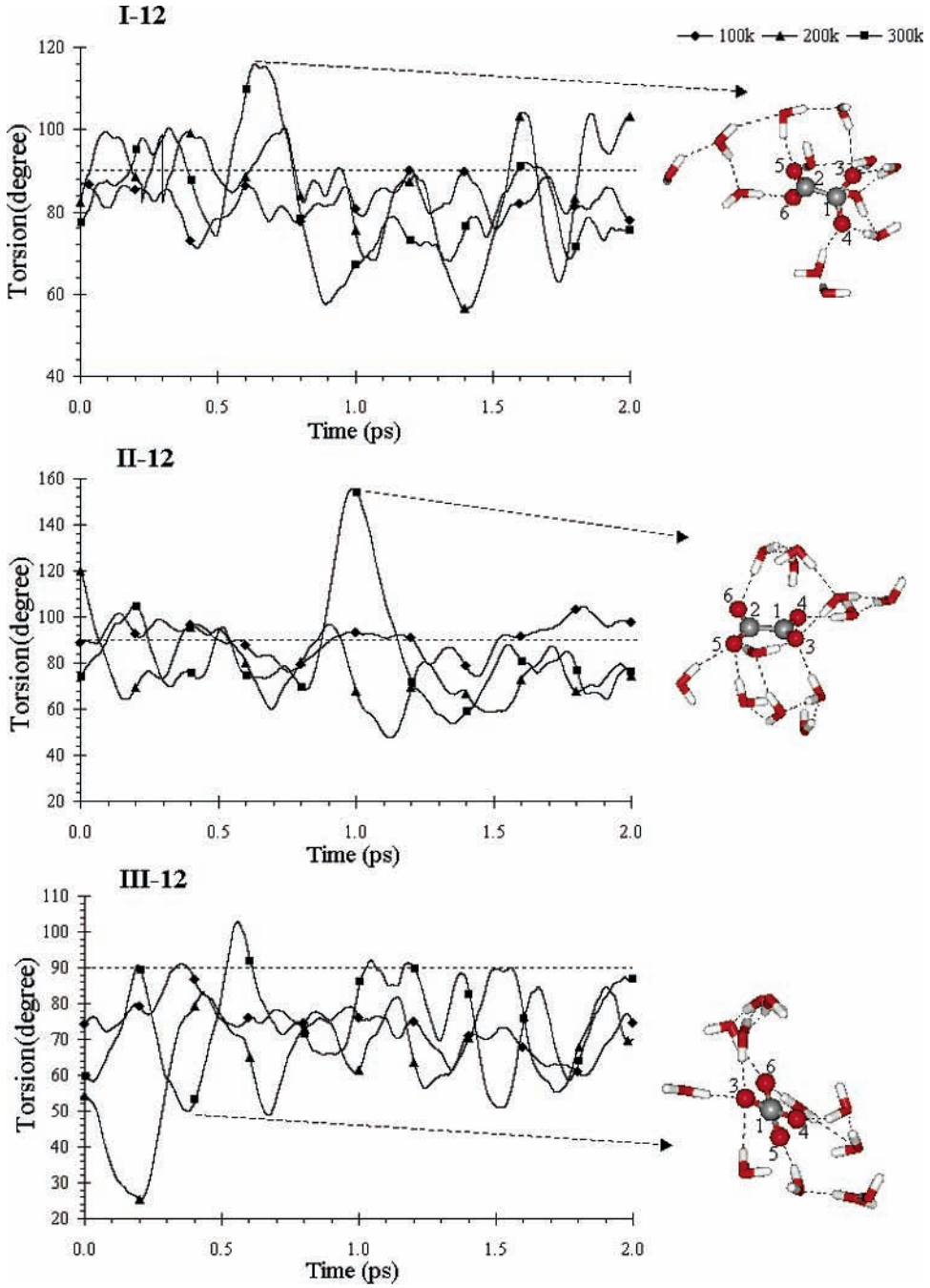

Figure 8. Variation of the C−C torsion angle in real time, for **I-12**, **II-12**, and **III-12**, as obtained by ab initio molecular dynamics simulations. Snapshot structures during the AIMD simulation are also shown for trajectory points with the largest deviation in C−C torsion angle from the expected value of 90°.

Though most of the H_2O molecules are in the first shell for **III-12** at 100 K, there is a tail centered around 4.4 Å. It is due to the back and forth movement of the four H_2O molecules on the side (O8, O14, O17, and O11 in Figure 1), whereas the two $(H_2O)_4$ are more stable. At 200 K, the side H_2O could become attached to the $(H_2O)_4$ ring, and the two rings could be opened during the simulation. Finally, at 300 K, the positions of H_2O molecules become scrambled.

One additional structural flexibility for $C_2O_4^{2-}(H_2O)_n$ is the torsion angle along the C−C bond. As shown in Figure 8, the fluctuation is substantial and, not surprisingly, increases in extent with increasing temperature. The solvation dynamics around $C_2O_4^{2-}$ is influenced not only by the fluctuation of solvent positions but also by the coupling between the torsional movement and solute−solvent interactions. Snapshot structures during the AIMD simulation for those torsion angles with the largest deviations from the standard value of 90° are also shown in Figure 8.

Summary

The structural evolution for anionic $C_2O_4^{2-}(H_2O)_n$, with $n = 6-12$, is similar to that for $SO_4^{2-}(H_2O)_n$ and distinct from the well studied structure of hydrated halide clusters. Although the symmetry of $C_2O_4^{2-}(H_2O)_n$ is less than that of $SO_4^{2-}(H_2O)_n$, the even distribution of negative changes around the four oxalate oxygen atoms still enforces a degree of symmetry in the solvation shell, and the $C_2O_4^{2-}$ group is at the center of the cluster. The maximum number of water molecules in the first shell is 12.

Although the two charges are separated in $C_2O_4^{2-}$ due to the presence of a C−C bond, extensive hydrogen bonding among the solvent molecules is observed. Stepwise solvation energy can reach 15 kcal/mol and decreases as n increases from 6 to 12. The larger space around $C_2O_4^{2-}$ makes it easier to accommodate both solute−solvent and solvent−solvent interactions, and as a result, the fluctuation in the solvation energy is considerably less than that observed for $SO_4^{2-}(H_2O)_n$.

"Crowding effects" are observed in ab initio molecular dynamics simulations at finite temperatures, similar to the case for $SO_4^{2-}(H_2O)_n$. The torsion angle along the C−C bond changes substantially during the simulation.

Acknowledgment. The work reported is supported by an Earmarked Grant (Project No. 401803) from the Research Grants Council of Hong Kong SAR Government. We are grateful for the generous allocation of computer time on the clusters of PCs and AlphaStations at the Chemistry Department, and the Center for Scientific Modeling and Computation, and on the high performance computing facilities at the Information Technology Service Center, all located at The Chinese University of Hong Kong.

References and Notes

(1) Marcus, Y. *Ion Solvation*; Wiley: New York, 1985.
(2) Dreuw, A.; Cederbaum, L. S. *Chem. Rev.* **2002**, *102*, 181.
(3) Simons, J.; Skurski, P.; Barrios, R. *J. Am. Chem. Soc.* **2000**, *122*, 11893.
(4) Boldyrev, A. I.; Simons, J. *J. Phys. Chem.* **1994**, *98*, 2298.
(5) Fenn, J. B.; Mann, M.; Meng, C. K.; Wong, S. F.; Whitehouse, C. M. *Science* **1985**, *246*, 64.
(6) Kebarle, P.; Tang, L. *Anal. Chem.* **1993**, *65*, A972.
(7) Blades, A. T.; Klassen, J. S.; Kebarle, P. *J. Am. Chem. Soc.* **1995**, *117*, 10563.
(8) Blades, A. T.; Kebarle, P. *J. Am. Chem. Soc.* **1994**, *116*, 10761.
(9) Wong, R. L.; Williams, E. R. *J. Phys. Chem. A* **2003**, *107*, 10976.
(10) Jurchen, J. C.; Garcia, D. E.; Williams, E. R. *J. Am. Soc. Mass Spectrosc.* **2003**, *14*, 1373.
(11) Wang, X. B.; Yang, X.; Nicholas, J. B.; Wang, L. S. *Science* **2001**, *294*, 1322.
(12) Wang, X. B.; Nicholas, J. B.; Wang, L. S. *J. Chem. Phys.* **2000**, *113*, 10837.
(13) Yang, X.; Wang, X. B.; Wang, L. S. *J. Phys. Chem. A* **2002**, *106*, 7607.
(14) Wang, X. B.; Yang, X.; Nicholas, J. B.; Wang, L. S. *J. Chem. Phys.* **2003**, *119*, 3631.
(15) Xantheas, S. S. *J. Phys. Chem.* **1996**, *100*, 9703.
(16) Gora, R. W.; Roszak, S.; Leszczynski, J. *Chem. Phys. Lett.* **2000**, *325*, 7.
(17) Robertson, W. H.; Johnson, M. A. *Annu. Rev. Phys. Chem.* **2003**, *54*, 173.
(18) Choi, J. H.; Kuwata, K. T.; Cao, Y. B.; Okumura, M. *J. Phys. Chem. A* **1998**, *102*, 503.
(19) Lee, H. M.; Kim, D. W.; Kim, K. S. *J. Chem. Phys.* **2002**, *116*, 5509.
(20) Gao, B.; Liu, Z. F. *J. Chem. Phys.* **2004**, *121*, 8299.
(21) Wang, X. B.; Nicholas, J. B.; Wang, L. S. *J. Chem. Phys.* **2000**, *113*, 653.
(22) Kambalapalli, S.; Ortiz, J. V. *J. Phys. Chem. A* **2003**, *107*, 10360.
(23) Herbert, J. M.; Ortiz, J. V. *J. Phys. Chem. A* **2000**, *104*, 11786.
(24) Dessent, C. E. H.; Rigby, C. *Chem. Phys. Lett.* **2003**, *370*, 52.
(25) Car, R.; Parrinello, M. *Phys. Rev. Lett.* **1985**, *55*, 2471.
(26) Cohen, M. L. *Phys. Rep.* **1984**, *110*, 293.
(27) Payne, M. C.; Teter, M. P.; Allan, D. C.; Arias, T. A.; Joannopoulos, J. D. *Rev. Mod. Phys.* **1992**, *64*, 1045.
(28) Tuckerman, M. E.; Ungar, P. J.; Vonrosenvinge, T.; Klein, M. L. *J. Phys. Chem.* **1996**, *100*, 12878.
(29) Kresse, G.; Hafner, J. *Phys. Rev. B* **1993**, *47*, 558.
(30) Kresse, G.; Hafner, J. *Phys. Rev. B* **1994**, *49*, 14251.
(31) Kresse, G.; Furthmüller, J. *Phys. Rev. B* **1996**, *54*, 11169.
(32) Kresse, G.; Furthmüller, J. *Comput. Mater. Sci.* **1996**, *6*, 15.
(33) Perdew, J. P. In *Electronic Structure of Solids '91*; Ziesche, P., Eschrig, H., Eds.; Academie Verlag: Berlin, 1991; p 11.
(34) Vanderbilt, D. *Phys. Rev. B* **1990**, *41*, 7892.
(35) Kresse, G.; Hafner, J. *J. Phys. Condens. Matter* **1994**, *6*, 8245.
(36) Kresse, G.; Hafner, J. *Phys. Rev. B* **1993**, *48*, 13115.
(37) Nosé, S. *J. Chem. Phys.* **1984**, *81*, 511.
(38) Hoover, W. *Phys. Rev. A* **1985**, *31*, 1695.
(39) Frisch, M. J.; Trucks, G. W.; Schlegel, H. B.; Scuseria, G. E.; Robb, M. A.; Cheeseman, J. R.; Zakrzewski, V. G.; Montgomery, J. A., Jr.; Stratmann, R. E.; Burant, J. C.; Dapprich, S.; Millam, J. M.; Daniels, A. D.; Kudin, K. N.; Strain, M. C.; Farkas, O.; Tomasi, J.; Barone, V.; Cossi, M.; Cammi, R.; Mennucci, B.; Pomelli, C.; Adamo, C.; Clifford, S.; Ochterski, J.; Petersson, G. A.; Ayala, P. Y.; Cui, Q.; Morokuma, K.; Malick, D. K.; Rabuck, A. D.; Raghavachari, K.; Foresman, J. B.; Cioslowski, J.; Ortiz, J. V.; Stefanov, B. B.; Liu, G.; Liashenko, A.; Piskorz, P.; Komaromi, I.; Gomperts, R.; Martin, R. L.; Fox, D. J.; Keith, T.; Al-Laham, M. A.; Peng, C. Y.; Nanayakkara, A.; Gonzalez, C.; Challacombe, M.; Gill, P. M. W.; Johnson, B. G.; Chen, W.; Wong, M. W.; Andres, J. L.; Head-Gordon, M.; Replogle, E. S.; Pople, J. A. *Gaussian 98*, revision a.11; Gaussian, Incorporated: Pittsburgh, PA, 1998.
(40) Kim, J.; Suh, S. B.; Kim, K. S. *J. Chem. Phys.* **1999**, *111*, 10077.
(41) Zhao, C. G.; Dixon, D. A. *J. Phys. Chem. B* **2003**, *107*, 4403.
(42) Rodriguez-Cruz, S. E.; Jockusch, R. A.; Williams, E. R. *J. Am. Chem. Soc.* **1999**, *121*, 1986.
(43) Rodriguez-Cruz, S. E.; Jockusch, R. A.; Williams, E. R. *J. Am. Chem. Soc.* **1999**, *121*, 8898.